NASA TECHNICAL NOTE

NASA TN D-6045

c. 1

NASA TN D-6045

BURNING OF SOLID ALUMINUM AND MAGNESIUM SPHERES IN HIGH-TEMPERATURE AND HIGH-VELOCITY GASES

by Robert D. Ingebo

Lewis Research Center

Cleveland, Ohio 44135

NATIONAL AERONAUTICS AND SPACE ADMINISTRATION • WASHINGTON, D. C. • OCTOBER 1970

1. Report No. NASA TN D-6045	2. Government Accession No.	3. Recipi
4. Title and Subtitle BURNING OF SOLID ALUMINUM AND MAGNESIUM SPHERES IN HIGH-TEMPERATURE AND HIGH-VELOCITY GASES		5. Report Date October 1970
		6. Performing Organization Code
7. Author(s) Robert D. Ingebo		8. Performing Organization Report No. E-5719
9. Performing Organization Name and Address Lewis Research Center National Aeronautics and Space Administration Cleveland, Ohio 44135		10. Work Unit No. 128-31
		11. Contract or Grant No.
		13. Type of Report and Period Covered Technical Note
12. Sponsoring Agency Name and Address National Aeronautics and Space Administration Washington, D.C. 20546		14. Sponsoring Agency Code
15. Supplementary Notes		

16. Abstract

The burning of solid aluminum and magnesium spheres (0.63-cm diam) in high-temperature and high-velocity gases, produced by the combustion of hydrogen and oxygen, was investigated experimentally. A range of combustion gas-stream velocities (6600 to 25 400 cm/sec), temperatures (1545° to 3198° C), and pressures (13.6 to 18.4 atm or 1.37×10^{5} to 1.86×10^{5} N/m^{2}) gave total burning times ranging from 125 to 355 msec. The time required to heat the surface of the sphere to the melting point was approximately one-half as long as the total burning time. Burning times were correlated with calculated values using a model based on a heat balance at the surface of the solid.

17. Key Words (Suggested by Author(s)) Metal combustion; Solid propellants; Burning magnesium spheres; Burning aluminum spheres	18. Distribution Statement Unclassified - unlimited

19. Security Classif. (of this report)	20. Security Classif. (of this page)	21. No. of Pages	22. Price*
Unclassified	Unclassified	23	$3.00

*For sale by the Clearinghouse for Federal Scientific and Technical Information Springfield, Virginia 22151

BURNING OF SOLID ALUMINUM AND MAGNESIUM SPHERES IN HIGH-TEMPERATURE AND HIGH-VELOCITY GASES

by Robert D. Ingebo

Lewis Research Center

SUMMARY

Burning of solid aluminum and magnesium spheres in high-temperature and high-velocity gases, produced by the combustion of hydrogen and oxygen, was investigated experimentally. Metal spheres were 0.63 centimeter in diameter, and the flow environment was varied to produce a Reynolds number of the sphere that varied from approximately 6000 to 31 000. Burning or erosion started at the front surface of the metal sphere. The entire burning process was divided into two phases; the initial phase, during which the sphere was heated to the melting temperature of the metal with no erosion, was called a heating period. The heating period was followed by erosion with combustion stabilized in the wake of the sphere.

The experimental heating and erosion times were correlated with Nusselt numbers by an equation derived from a model using a heat balance at the surface of the solid. The heat balance equation was based on the Reynolds and Nusselt numbers of the initial sphere because it was observed that the erosion rate was constant as the mass of the metal or effective diameter decreased.

INTRODUCTION

Rapid and efficient burning of high-energy fuels such as aluminum and magnesium is difficult to achieve. This is primarily due to combustion-inhibiting processes inherent in metal-fuel combustion. However, metal fuels still appear promising as a source of power. They have been used primarily as additives in solid-fueled rocket engines to improve the specific impulse and stability.

Considerable effort has been made to determine the combustion mechanism for metals in quiescent oxidizing gases (refs. 1 to 3). Also, data have been obtained on the combustion of slurry fuels in jet engines (ref. 4). However, very little data is available on metal burning rates under actual combustor conditions and the influence of metals on combustion stability. The development of metal-fueled combustors requires new techniques of injecting, rapidly igniting, and burning metal particles to efficiently control the burning process.

In this investigation of metal fuels, the main purpose was to determine mass and temperature histories of relatively large (0.63-cm diam) aluminum and magnesium spheres burning under simulated rocket combustor conditions. Such data are needed to derive a combustion model that could describe the actual burning process for metal fuels in a rocket engine and possibly explain the influence of metal additives in controlling combustion instability.

SYMBOLS

c_p	specific heat, g-cal/(g)(^{o}C); J/(g)(^{o}C)
D_t	nozzle throat diameter, cm
d	sphere diameter, cm
dm/dt	erosion rate, g/sec
H_f	latent heat of fusion, g-cal/g; J/g
h	heat-transfer coefficient, g-cal/(sec)(cm^2)(^{o}C); J/(sec)(cm^2)(^{o}C)
k	thermal conductivity, g-cal/(sec)(cm^2)(^{o}C/cm); J/(sec)(cm^2)(^{o}C/cm)
m	sphere weight, g
Nu	Nusselt number, hd/k_g
o/f	mass mixture ratio of oxidant to fuel
P	pressure, psia; N/m^2 abs
Pr	Prandtl number, $\mu_g c_{p,g}/k_g$
q	heat-transfer rate, g-cal/sec; J/sec
Re	Reynolds number based on sphere diameter, $dV_g\rho_g/\mu_g$
r	sphere radius, cm
T	temperature, ^{o}C
t	time, sec

V	velocity, cm/sec
α_1	absorptivity
α_2	emissivity
μ	fluid viscosity, P; (N)(sec)/m^2
ρ	fluid density, g/cm^3
σ	Stefan-Boltzmann constant

Subscripts:

avg	average for sphere lifetime
C	sphere center
c	convection
e	erosion
fs	front surface
g	gas
i	initial
m	metal
mp	melting point
r	radiation
s	surface
t	total

Superscripts:

—	average
'	approximate

APPARATUS AND PROCEDURE

A rocket combustor, shown in figure 1, was used to determine burning histories of solid 0.63-centimeter-diameter aluminum and magnesium spheres inserted into high-velocity and high-temperature gases. The gas stream was produced by burning gaseous hydrogen and liquid oxygen injected 46 centimeters upstream of the spheres at mass mixture ratios of oxidant to fuel o/f of 1.7, 5.3, 8, 10, and 12. Three different exhaust

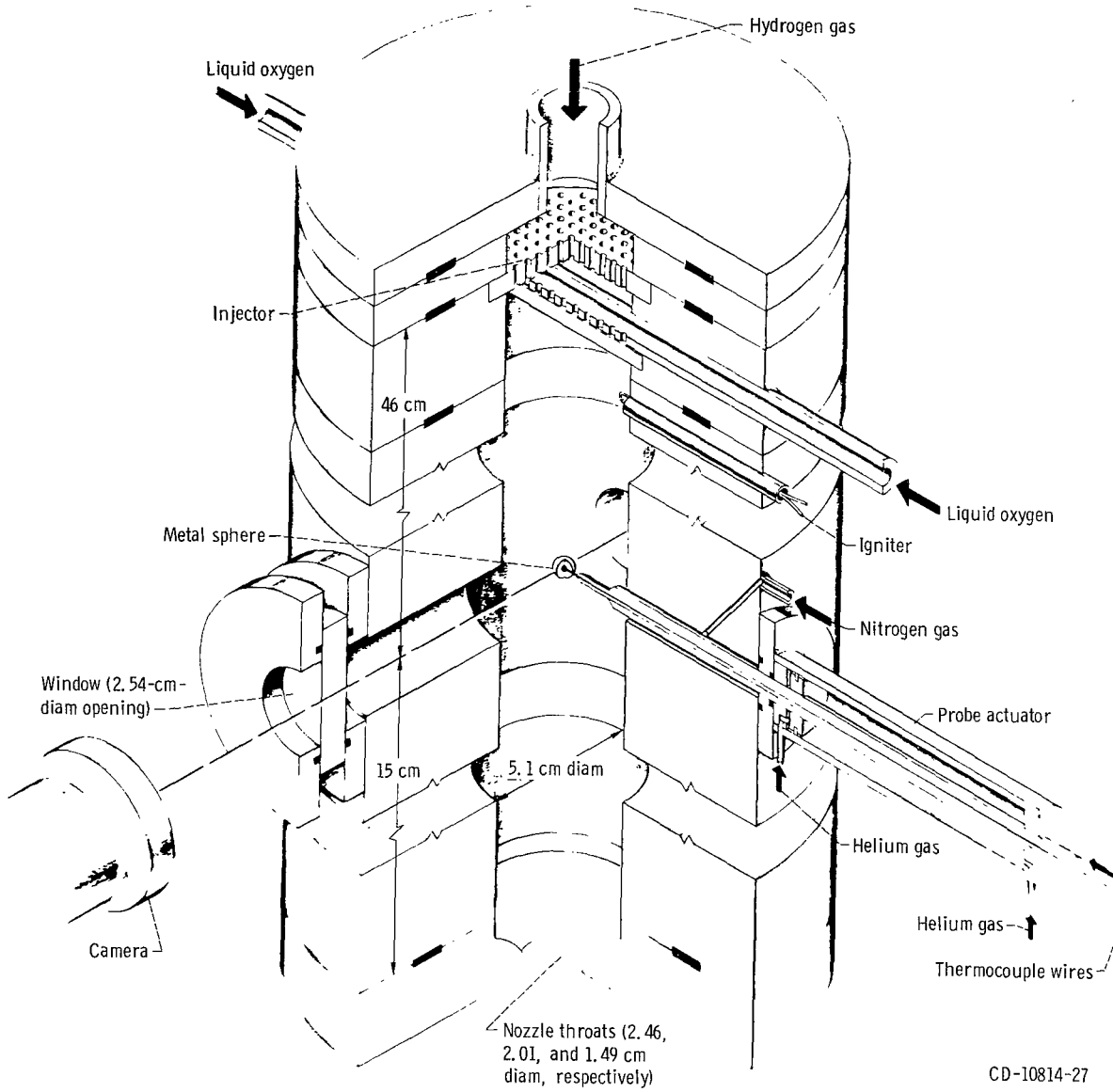

Figure 1. - Diagram of rocket combustor and auxiliary equipment.

nozzles were used having throat diameters of 2.46, 2.01, and 1.49 centimeters, which gave a combustion gas-stream velocity range of 6600 to 25 400 centimeters per second. These operating conditions resulted in a Reynolds number for the metal sphere ranging between 6000 and 31 000. At a given o/f condition, the chamber pressure was approximately the same (within ±5 percent) for the three exhaust nozzle test conditions. Chamber pressures varied between 13.6 and 18.4 atmospheres (1.37×10^5 and 1.86×10^5 N/m^2) with different mixture ratios.

Spheres of aluminum (type 6061, 98 percent pure) and magnesium (type AZ31B, 97 percent pure) were machined from 1/4-inch (0.635-cm) rods. A hole was drilled and tapped to the center of the sphere for mounting on a 1/16-inch (0.159-cm) threaded stainless-steel rod. The spheres were mounted on the ceramic-coated tip of the probe, as shown in figure 1, and rapidly inserted into the center of the test section after equilibrium conditions had been obtained in the combustor. The tests were terminated by rapidly withdrawing the sphere back into the sheltered region cooled by nitrogen gas flow. The time measurement for each test began when the sphere passed out through the opening in the combustor wall and ended when it passed back through the same opening. The time required for the actuator to move the sphere 5.1 centimeters was 2 milliseconds for either insertion or withdrawal.

An iron-constantan thermocouple (0.0127-cm-diam wire) was mounted in the center of the sphere to determine its temperature history at that point ($r = 0$). In obtaining mass histories, the quantity of metal eroded from the sphere was determined by weighing the sphere before and after each burning test. Attempts to determine the weight loss of a sphere by photographing it as it burned inside of the combustor proved unsuccessful since erosion was very nonuniform over its surface.

RESULTS AND DISCUSSION

A typical set of data showing mass and temperature histories of an aluminum sphere is plotted in figure 2(a). Actually, seven spheres weighing 0.350±0.003 gram were tested under identical conditions to obtain the complete history of a single sphere. One of the spheres was instrumented with a thermocouple junction installed in the center of the sphere to obtain the temperature history T_C as a function of time t. In the case of aluminum (fig. 2(a)), the temperature at the center rose from the initial temperature of 20° C to the melting point (660° C) in approximately 250 milliseconds and then remained constant. In the case of magnesium (fig. 2(b)), the temperature at the center of the sphere rose to a constant value considerably below the melting point of magnesium in approximately 150 milliseconds.

Figure 2(a) also shows the mass history of an aluminum sphere. At approximately 170 milliseconds after the sphere was inserted into the gas stream, it was observed, both photographically during the run and visually by inspecting the withdrawn sphere, that erosion was just beginning to occur at the front surface. Erosion at this surface is believed to be due to the fact that the heat-transfer coefficient was considerably greater at the front surface than at the rear surface of the sphere. This is shown by the plots of calculated values of the front surface temperature T_{fs} against time t and the average surface temperature $\overline{T}_s$ against time t in figure 2(a). Thus, in 170 milliseconds, the

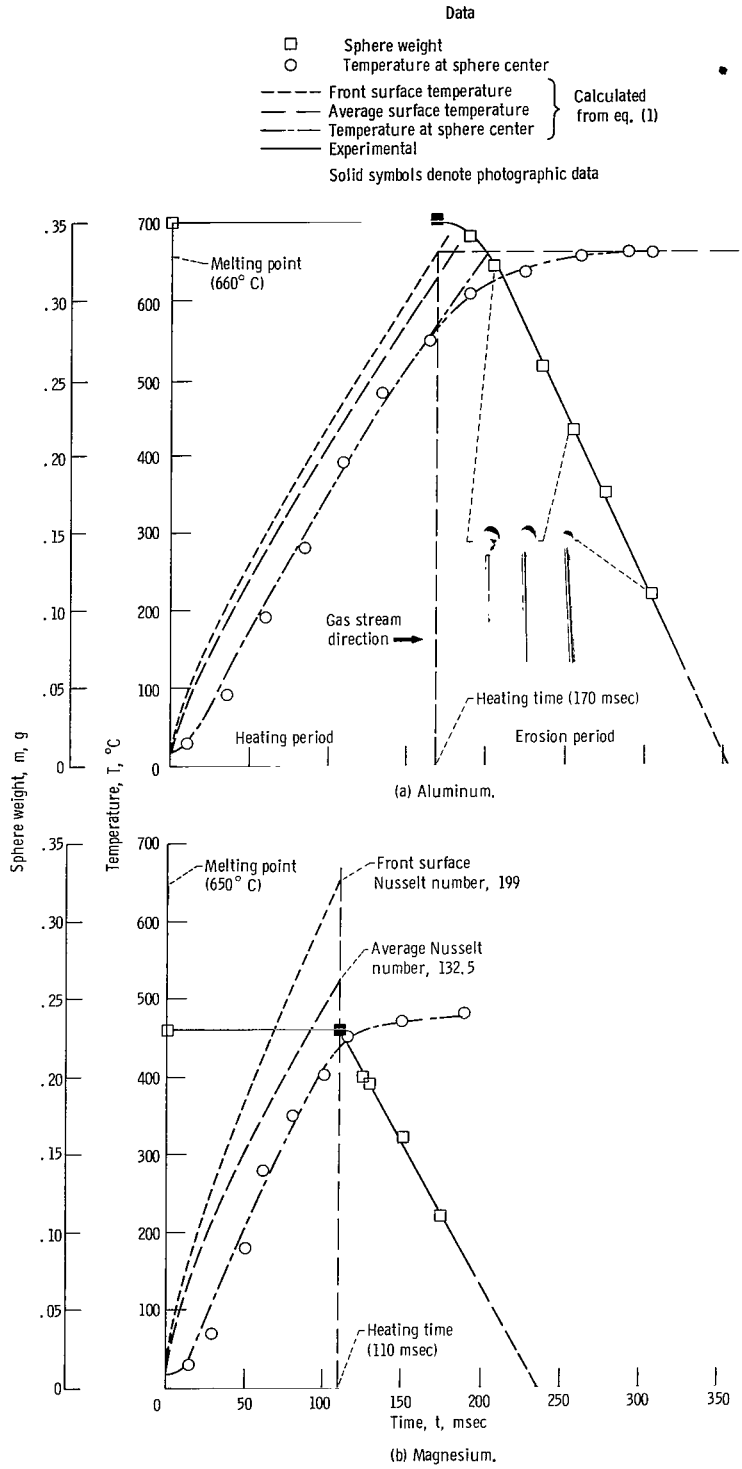

Figure 2. - Weight and temperature histories of 0.63-centimeter-diameter aluminum and magnesium spheres. Mass mixture ratio of oxidant to fuel, 1.7; nozzle throat diameter, 2.01 centimeters.

front surface temperature reached the melting point (660° C), whereas the calculated average surface temperature was 30° below the melting point.

Spheres withdrawn at 205, 255, and 305 milliseconds are shown in figure 2(a). These photographs indicate that erosion was considerably greater at the front than at the rear of the sphere because of the higher heat-transfer coefficient at the leading surface. As a result, the metal spheres did not remain spherical during the erosion period. The mass history of the sphere showed that shortly after erosion began (called ignition) its weight decreased linearly with time.

Heating of Metal Spheres

Data on the sphere heating rate and the time required for it to reach the melting point at the front surface were analyzed in the following manner.

Heating rates. - The heating rate was calculated by writing a heat balance at the surface of the metal sphere as

$$q_m = q_{g,c} = \pi r^2 k_m \left.\frac{dT}{dr}\right|_{r=r_s} \tag{1}$$

where q_m is the heating rate of the sphere and $q_{g,c}$ is the rate of heat transfer by convection from the gas stream. Heat transferred by radiation was negligible (approx 2 percent of $q_{g,c}$). As discussed in appendix A, the change in sphere temperature with time was obtained from equation (1) by simultaneously solving equations (A1) and (A3) at the desired radii ($r = 0$ and $r = r_s$).

Values of the heat-transfer coefficient were assumed to calculate several temperature histories of the sphere. The best results shown in figure 2 were obtained with a heat-transfer coefficient h of 0.202 gram-calorie per second per square centimeter per $^{\circ}$C (0.847 J/(sec)(cm^2)($^{\circ}$C)). Both figures show that agreement was good between calculated and experimental values of the temperature at the center of the sphere T_c. Also shown in figure 2 are values of $\overline{T}_s$, the average surface temperature of the sphere.

Values of the average heat-transfer coefficient $\overline{h}$ are given in table I for a range of o/f conditions and corresponding values of the average Nusselt number, the Prandtl number, and the Reynolds number. The aluminum and magnesium spheres were tested at five different o/f conditions. Combustion gas properties used in these calculations are discussed in appendix B. Gas velocities used for these tests are given in table II for a nozzle throat diameter D_t of 2.01 centimeter.

TABLE I. - CALCULATED VALUES FOR HEAT-TRANSFER RATES

[Nozzle throat diameter, 2.01 cm.]

Mass mixture ratio of oxidant to fuel, o/f	Temperature of gas, T_g, ^oC	Average heat-transfer coefficient, $\bar{h}$		Average Nusselt number, $\overline{Nu}$	Prandtl number, Pr	Reynolds number, Re
		g-cal/(sec)(cm^2)(^oC)	J/(sec)(cm^2)(^oC)			
1.7	1545	0.2020	0.848	132.5	0.526	21 000
5.3	2977	.1295	.543	93.0	.595	12 130
8	3198	.0967	.406	94.0	.758	10 850
10	3144	.0904	.379	98.5	.744	10 400
12	3054	.0812	.341	94.5	.734	10 380

TABLE II. - EXPERIMENTAL RESULTS

Nozzle throat diameter, D_t, cm	Mass mixture ratio of oxidant to fuel, o/f	Velocity of gas, V_g, cm/sec	Reynolds number, Re	Average Nusselt number, $\overline{Nu}$	Magnesium				Aluminum			
					Heating time, t_s, msec	Average surface temperature, $\overline{T}_s$, ^oC	Average erosion rate, $(dm/dt)_{avg}$, g/sec		Heating time, t_s, msec	Average surface temperature, $\overline{T}_s$, ^oC	Average erosion rate, $(dm/dt)_{avg}$, g/sec	
							Experimental	Calculated (eq. (10))			Experimental	Calculated (eq. (10))
1.49	1.7	9 270	11 500	90.5	175	555	1.48	1.42	---	---	----	----
	5.3	8 150	6 650	67.7	115	540	2.50	2.64	---	---	----	----
	8	7 530	5 950	67.3	140	524	1.84	1.78	---	---	----	----
	10	6 830	5 700	65.5	160	497	1.54	1.44	---	---	----	----
	12	6 580	5 680	65.3	170	479	1.32	1.26	---	---	----	----
2.01	1.7	16 900	21 000	132.5	110	525	1.84	2.02	170	630	2.07	2.29
	5.3	14 850	12 130	93.0	80	526	2.80	3.05	120	620	3.27	3.63
	8	13 730	10 850	94.0	90	493	2.15	2.34	150	610	2.89	2.91
	10	12 450	10 400	98.5	95	476	2.00	2.06	160	603	2.71	2.61
	12	12 000	10 380	98.3	100	450	1.77	1.78	175	595	2.43	2.31
2.46	1.7	25 400	31 600	169.5	90	520	2.23	2.56	135	625	3.12	2.94
	5.3	22 300	18 200	123.5	60	497	3.54	3.83	95	614	4.38	4.85
	8	20 600	16 300	125.0	70	481	3.08	3.03	115	600	3.76	3.88
	10	18 700	15 600	118.5	75	447	2.38	2.65	125	592	3.36	3.15
	12	18 000	15 570	118.5	80	431	2.30	2.08	135	585	3.07	2.70

The heat-transfer coefficients were correlated with the dimensionless groups as follows: McAdams (ref. 5) relates the heat-transfer coefficient for solid spheres at large Reynolds numbers with the Nusselt number and Reynolds number as

$$\frac{\bar{h}d}{k_g} = \overline{Nu} = 0.37\ Re^{0.6} \tag{2}$$

However, the theoretical minimum value for the Nusselt number is 2 (when $Re = 0$). Heat-transfer relations have also generally shown that $Nu \sim Pr^{0.3}$. Therefore, the preceding expression was modified to

$$\overline{Nu} = 2 + CPr^{0.3}Re^{0.6} \tag{3}$$

where C is a proportionality constant. To evaluate C, data in table I were plotted as shown in figure 3, and the following expression was obtained for solid spheres:

$$\overline{Nu} = 2 + 0.4\ Pr^{0.3}Re^{0.6} \tag{4}$$

Properties used in equations (2) to (4) are evaluated at the mean temperature of the combustion gases and surface and for static pressures.

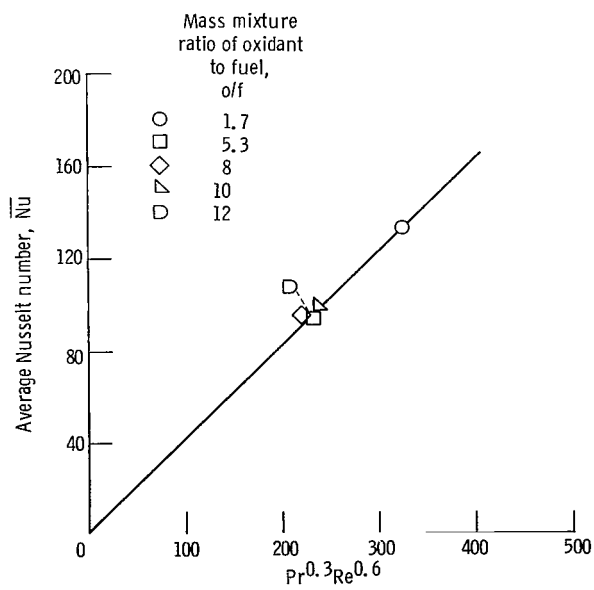

Figure 3. - Correlation of Nusselt number with Prandtl and Reynolds numbers.

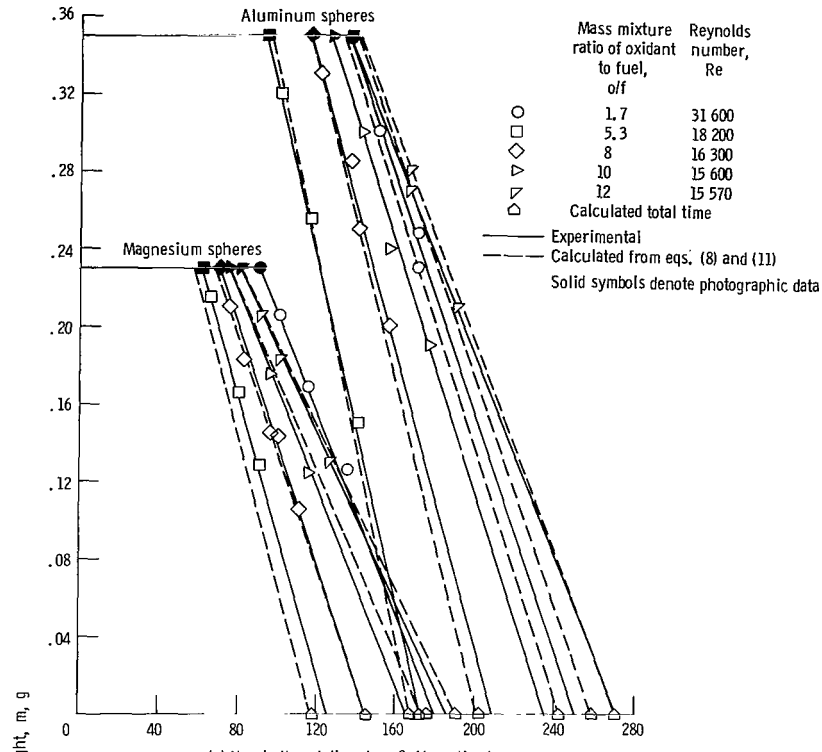

(a) Nozzle throat diameter, 2.46 centimeters.

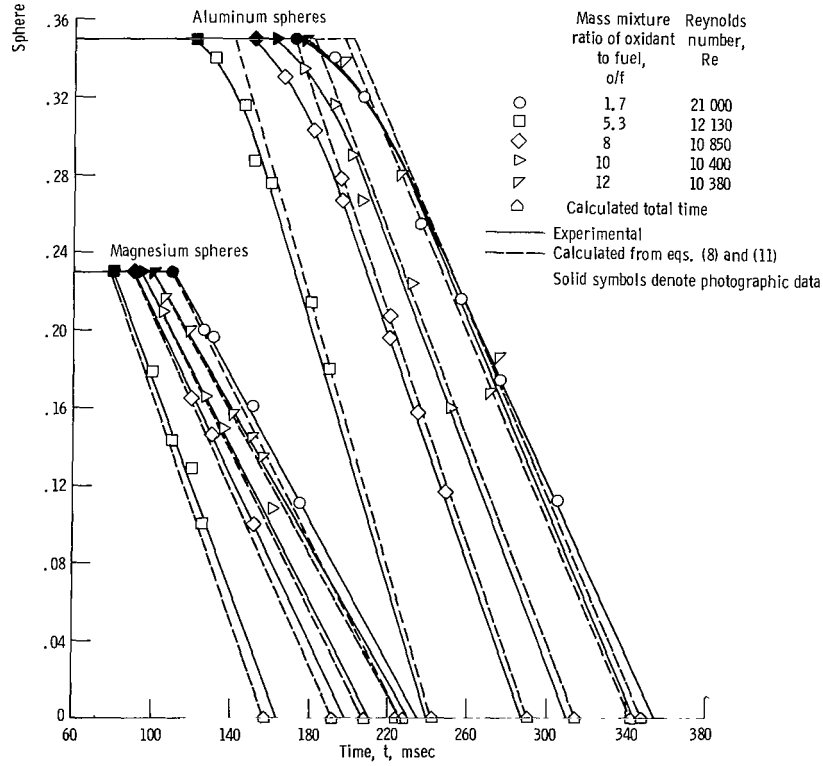

(b) Nozzle throat diameter, 2.01 centimeters.

Figure 4. - Erosion histories.

Heating times. - From high-speed motion pictures of the spheres, it was observed that melting first occurred at the front surface. Thus, the heating time t_s was determined photographically from the time of insertion of the sphere into the gas stream to the time that melting was first observed at the front surface. Experimental values of the heating time t_s are recorded in table II and plotted as the solid symbols in figure 4 at the breakpoint in the mass history of the sphere.

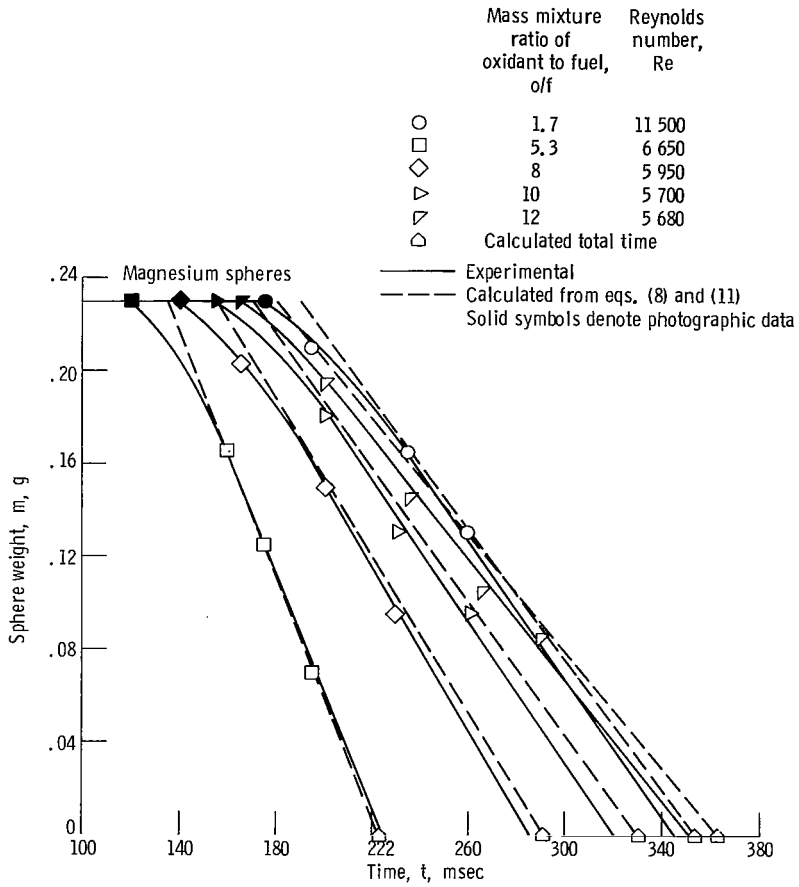

(c) Nozzle throat diameter, 1.49 centimeters.

Figure 4. - Concluded.

In order to calculate the heating time t_s from the heating rate (eq. (1) or (A1) and (A3)), it is necessary to know the average surface temperature $\overline{T}_s$ at the time t_s (when $T_{fs} = T_{mp}$). The average surface temperature when melting first occurred varied with flow conditions. Therefore, it was assumed that the nondimensional temperature ratio $\overline{T}_s/T_{mp}$ was a function of the average Nusselt number. Also, $\overline{T}_s$ was considerably lower

for magnesium than it was for aluminum, at the same value of $\overline{Nu}$. Consequently, it was also assumed that $\overline{T}_s/T_{mp}$ was a function of the ratio of gas to liquid-metal density ρ_g/ρ_m. The following expression was therefore assumed for calculating $\overline{T}_s$ at the time t_s:

$$\frac{T_{mp}}{\overline{T}_s} = 1 + C(\overline{Nu})^m\left(\frac{\rho_g}{\rho_m}\right)^n \tag{5}$$

This is an empirical correlation that might not be valid for other metals.

The exponent m was evaluated by plotting $(T_{mp}/\overline{T}_s) - 1$ against $\overline{Nu}$ (as shown in fig. 5), and m was found to be 0.7. Similarly, a plot of $(T_{mp}/\overline{T}_s^{-1})\overline{Nu}^{-0.7}$ against ρ_g/ρ_m

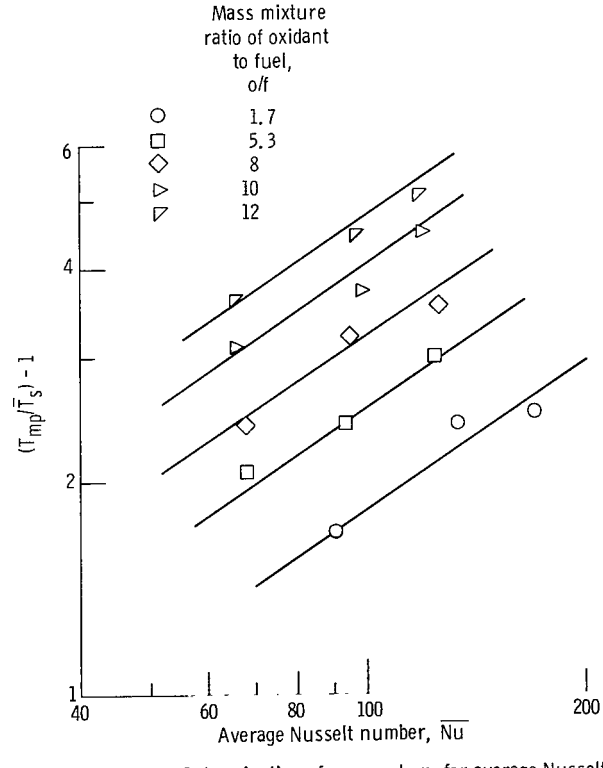

Figure 5. - Determination of exponent m for average Nusselt number.

(shown in fig. 6), gave an n of 3. Finally, $T_{mp}/\overline{T}_s$ was plotted against $Nu^{0.7}(\rho_g/\rho_m)^3$ (fig. 7), and the proportionality constant C was determined to be 1.1×10^8. Thus, equation (5) was rewritten as

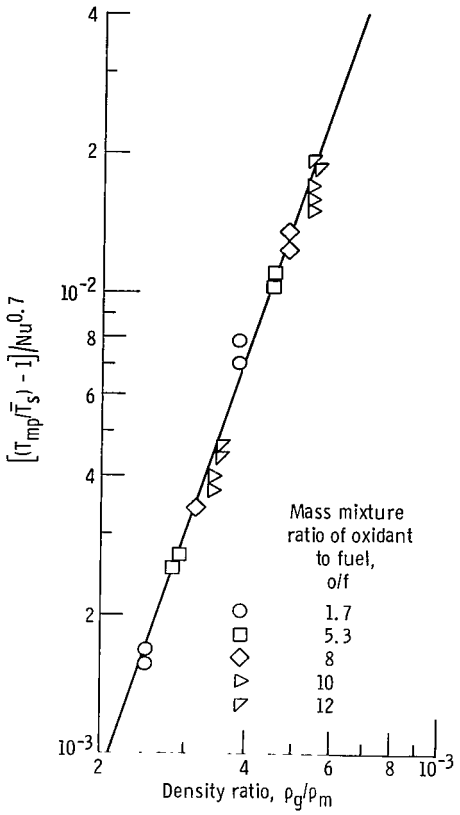

Figure 6. - Determination of exponent n for density ratio.

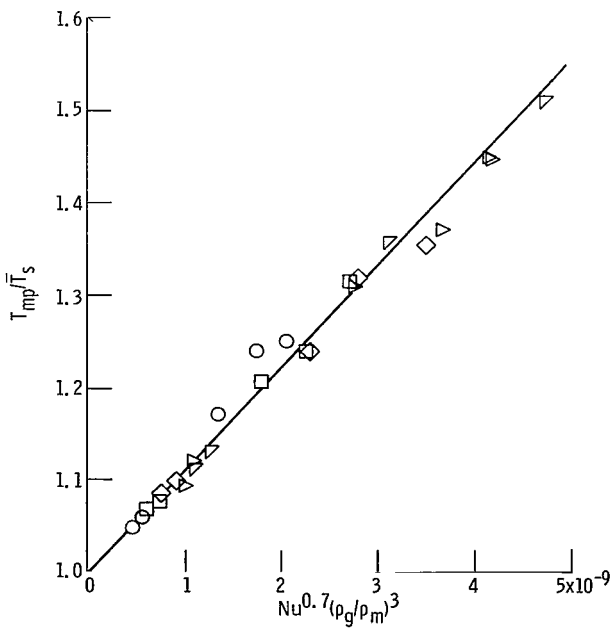

Figure 7. - Determination of proportionality constant C in equation (4).

$$\frac{T_{mp}}{\overline{T}_s} = 1 + 1.1\times10^8\ Nu^{0.7}\left(\frac{\rho_g}{\rho_m}\right)^3 \tag{6}$$

which gives the average surface temperature $\overline{T}_s$ when the leading edge reaches the melting temperature, defined as the end of the heating time t_s. This is the time at which heating ends and erosion begins.

Although machine calculations using equations (1) and (6) were used to determine t_s at $\overline{T}_s$, a simpler method was derived from the following heat balance at the surface of the sphere:

$$\pi d_i k_g (T_g - \overline{T}_s)\overline{Nu}_i = m c_{p,s}\left(\frac{T_m}{\overline{T}_s}\right)\frac{d\overline{T}_s}{dt} \tag{7}$$

which may be integrated to give

$$t_s' = \frac{m c_{p,s} T_m}{\pi d_i k_g \overline{Nu}_i \overline{T}_s} \ln \frac{T_g - T_i}{T_g - \overline{T}_s} \tag{8}$$

TABLE III. - COMPARISON BETWEEN CALCULATED AND EXPERIMENTAL RESULTS FOR MAGNESIUM AND ALUMINUM SPHERES

[Nozzle throat diameter, 2.01 cm.]

Metal	Mass mixture ratio, o/f	Heating time, msec		Erosion time, t_e, msec		Total time, t_t, msec	
		Approximate, t_s'	Experimental, $(t_s)_{exp}$	Equation (11)	Experimental	Calculated	Experimental
Magnesium	1.7	111	110	114	125	225	235
	5.3	80	80	76	83	156	163
	8	92	90	99	108	191	198
	10	95	95	112	115	207	210
	12	98	100	130	130	228	230
Aluminum	1.7	174	180	153	174	327	354
	5.3	125	120	97	120	222	240
	8	150	150	120	138	270	288
	10	161	160	134	150	295	310
	12	171	175	151	169	322	344

where t_s' is the approximate heating time and T_i is the initial sphere temperature. The agreement between values of t_s', calculated from equation (8), and experimental values of t_s was good, as shown in table III. Thus, t_s' is the approximate heating time required for the average surface temperature to reach $\overline{T}_s$ and erosion to begin.

Erosion of Metal Spheres

Motion pictures and eroded spheres indicated that molten metal was stripped from the surface of the sphere by the high-velocity gas stream and that the atomized liquid was vaporized and ignited, and combustion was stabilized in the wake of the sphere. A model for this erosion process is shown in figure 8.

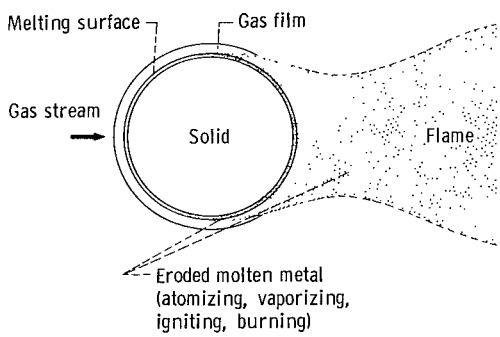

Figure 8. - Combustion model for eroding metal spheres.

In this portion of the study, the main objective was to determine erosion (mass removal) rates at the surface of the sphere and to compare them with calculated values. Calculations were made based on a heat balance and mass balance at the surface of the sphere. The use of a mass balance proved unsuccessful since the mass removal or erosion rate was not limited by the diffusion rate of oxidant gases to the surface of the sphere. Thus, a heat balance at the surface of the sphere was used to analyze the erosion data.

Erosion rates. - Applying a heat balance at the surface to the erosion of a metal sphere in high-temperature and high-velocity gas streams gives

$$q_L = q_g \tag{9}$$

where q_L is the rate at which heat is gained by the eroding liquid and q_g is the rate of heat transfer from the gas stream. In deriving this expression, the heating rate of the

metal was assumed to be negligible since it decreased rapidly when erosion began, and heat transfer from the flame was assumed negligible. Figure 4 shows that the average erosion rate $(dm/dt)_{avg}$ remained approximately constant with time. This result was attributed to the fact that as the metal eroded it did not remain spherical in shape. Thus, $\overline{Nu}$ could not be accurately determined during erosion. In fact, the curvature of the front surface became less convex, which tended to increase the front surface Nusselt number although the sphere diameter decreased with time. Therefore, the initial Nusselt number before erosion started was used to define the heat transfer to the surface during erosion. Because of the nonuniformity of the surface temperature of the sphere, the average value of the surface temperature $\overline{T}_s$ was used to evaluate the sensible heat gained by the metal as it was melted and eroded by the gas stream. Thus, $\overline{T}_s$ was also used to evaluate the temperature drop across the gas film surrounding the sphere. A heat balance at the surface of the sphere was written as

$$\left(\frac{dm}{dt}\right)_{avg}\left[H_f + c_{p,m}(T_{mp} - \overline{T}_s)\right] = \pi d_i k_g (T_g - \overline{T}_s)\overline{Nu}_i \tag{10}$$

where $(dm/dt)_{avg}$ is the average erosion rate, H_f is the heat of fusion of the metal, and d_i and $\overline{Nu}_i$ are the diameter and average Nusselt number, respectively, based on the initial sphere diameter. Values of $(dm/dt)_{avg}$ were calculated from equation (10) and plotted as shown in figure 4.

Erosion times. - The erosion time t_e may be obtained by integrating equation (10):

$$t_e = \frac{\rho_i d_i^2\left[H_f + c_{p,m}(T_{mp} - \overline{T}_s)\right]}{6k_g(T_s - \overline{T}_s)\overline{Nu}_i} \tag{11}$$

Values of t_e calculated from this equation agree reasonably well with experimental values of t_e, as shown in table III.

Total heating and erosion time. - The total time required for heating and erosion of metal spheres can be calculated from

$$t_t = t_s' + t_e \tag{12}$$

By substituting equations (8) and (11) into equation (12), the following expression was obtained:

$$t_t = \frac{\rho_L d_i^2 c_{p,m}}{6k_g \overline{Nu}_i} \left[\frac{T_{mp}}{\overline{T}_s} \ln \left(\frac{T_g - T_i}{T_g - T_s} \right) + \frac{H_f + c_{p,m}(T_{mp} - \overline{T}_s}{c_{p,m}(T_g - \overline{T}_s)} \right] \tag{13}$$

A comparison of values of t_t calculated from equation (13) and experimental values is shown in figure 4 and table III. Although no direct comparison could be made with the data given by Maček in reference 6, it could be assumed that $\overline{Nu} \simeq 2$ for the 0.0032 centimeter diameter aluminum sphere. This gives $t_t = 1.26$ milliseconds, which agrees fairly well with his data.

Burning Process with Eroding Metal Spheres

High-speed motion pictures of the spheres showed that soon after erosion was initiated the molten metal ignited and combustion was stabilized in the downstream wake of the sphere. A combustion model illustrating this burning with solid spheres is shown in figure 8. As this burning model indicates, there was no evidence of solid-phase combustion at the surface of the sphere, and no oxide shell was formed that would inhibit erosion or burning. The eroded molten metal appeared to be vaporizing and combustion was stabilized in the wake of the sphere with no appreciable amount of heat being transferred from the flame to the surface of the sphere. The luminosity of the flame was greatly increased when the erosion rate was increased and also when the o/f was increased.

SUMMARY OF RESULTS

The burning of solid aluminum and magnesium spheres (0.63-cm diam) in high-temperature and high-velocity gases, produced by the combustion of hydrogen and oxygen, has shown the following:

1. The front surface of a metal sphere was heated to its melting point before it began to erode and burn. There was no evidence of solid-phase burning at the surface of the sphere, and therefore no oxide shell was formed to inhibit the erosion process. Metal combustion was stabilized in the wake of the sphere and did not appreciably affect the erosion rate by transferring heat to the surface of the sphere.

2. Experimental heating and erosion times agreed well with values calculated from a heat balance at the surface of the sphere. The heating time for a metal sphere was approximately one-half as long as the total time required for complete erosion of the sphere.

3. The total burning time t_t (heating time plus erosion time) was correlated with the average Nusselt number $\overline{Nu}$:

$$t_t = \frac{\rho_m d_i^2 c_{p,m}}{6kg\overline{Nu}} \left[\frac{T_m}{\overline{T}_s} \ln\left(\frac{T_g - T_i}{T_s - \overline{T}_s} \right) + \frac{H_f + c_{p,m}(T_{mp} - \overline{T}_s)}{c_{p,m}(T_g - \overline{T}_s)} \right]$$

where ρ_m is the fluid density of the metal, d_i is the initial sphere diameter, $c_{p,m}$ is the specific heat of the metal, k_g is the thermal conductivity of the gas, T_m is the temperature of the metal, $\overline{T}_s$ is the average surface temperature of the sphere, T_g is the temperature of the gas, T_i is the initial temperature of the metal, H_f is the latent heat of fusion, and T_{mp} is the melting point of the metal.

4. The average surface temperature of the sphere $\overline{T}_s$ was correlated with the average Nusselt number $\overline{Nu}$ and the ratio of gas to liquid-metal density ρ_g/ρ_m:

$$\frac{T_{mp}}{T_s} = 1.0 + 1.10\times10^8 \, Nu^{0.7} \left(\frac{\rho_g}{\rho_m} \right)^3$$

5. The following correlation of the average Nusselt number with the Prandtl and Reynolds numbers was obtained:

$$\overline{Nu} = 2 + 0.4 \, Pr^{0.3} Re^{0.6}$$

This agreed well with data in the literature for heat transfer from air streams to solid spheres.

Lewis Research Center,
National Aeronautics and Space Administration,
Cleveland, Ohio, June 11, 1970,
128-31.

APPENDIX A

HEATING OF SOLID METAL SPHERES IN GAS STREAMS

The conduction of heat in a solid metal sphere may be expressed in spherical coordinates as

$$\frac{k_m}{\rho_m c_{p,m}} \frac{1}{r^2} \frac{\partial}{\partial r}\left(r^2 \frac{\partial T}{\partial t}\right) = \frac{\partial T}{\partial t} \tag{A1}$$

where $k_m/\rho_m c_{p,m}$ is the thermal diffusivity or ratio of the thermal conductivity to the product of the density and specific heat of the sphere and r is the radial distance of a point from the center of the sphere at temperature T and time t.

The heat balance at the surface of a metal sphere suspended in a high-temperature and high-velocity gas stream may be written as

$$q_m = g_{g,c} + q_{g,r} \tag{A2}$$

where q_m is the heating rate of the sphere and $q_{g,c}$ and $q_{g,r}$ are rates of heat transfer from the gas stream by convection and radiation, respectively. Since

$$q_m = \pi r^2 k_m \frac{dT}{dr}$$

$$q_{g,c} = \pi r^2 h(T_g - T_s)$$

and

$$q_{g,r} = \pi r^2\left(\alpha_1 T_g^4 - \alpha_2 T_s^4\right)$$

equation (A2) becomes

$$\left.\frac{dT}{dr}\right|_{r=r_s} = \frac{h}{k_m}(T_g - T_s) + \frac{\sigma}{k_m}\left(\alpha_1 T_g^4 - \alpha_2 T_s^4\right) \tag{A3}$$

where h is the heat-transfer coefficient at the surface of the sphere, σ is the Stefan-Boltzmann constant, and α_1 and α_2 are the absorptivity and emissivity of the polished metal, respectively.

APPENDIX B

COMBUSTION GAS PROPERTIES

Combustion gas properties were calculated for equilibrium conditions in the combustor by the method given in reference 6. The results are given in table IV for the three exhaust nozzles used in this study.

The viscosity and thermal conductivity of the combustion gas stream were also determined by this method for a range of gas temperatures. The results of these calculations are plotted in figure 9.

TABLE IV. - COMBUSTION GAS STREAM PROPERTIES

Mass mixture ratio, o/f	Gas pressure, P_g		Gas temperature, T_g, °C	Gas density, ρ_g, g/cm^3
	psia	N/m^2 abs		
1.7	270	18.6×10^5	1818	6.70
5.3	255	17.5	3250	7.92
8	230	15.8	3471	8.58
10	215	14.8	3417	9.18
12	200	13.7	3327	9.57

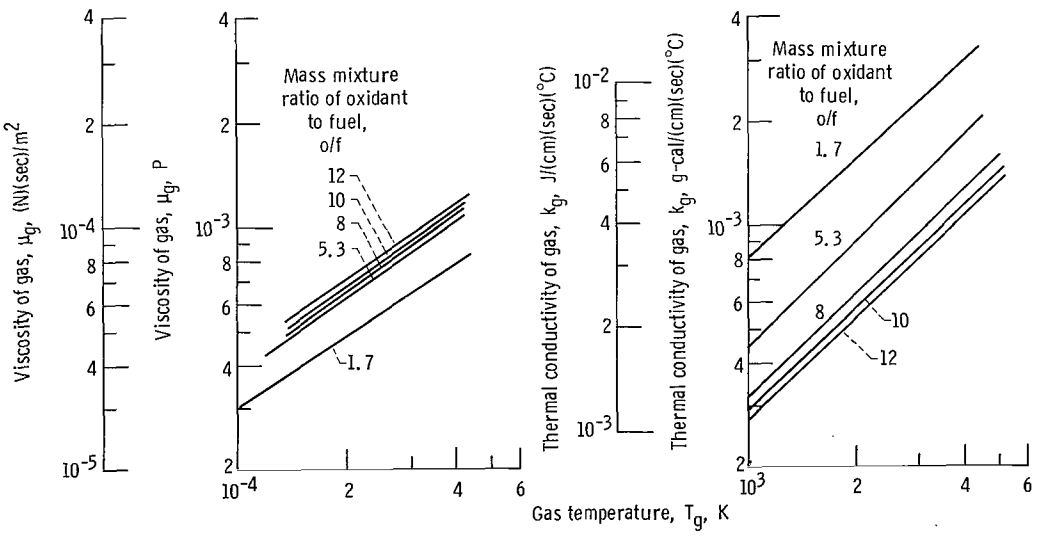

Figure 9. - Combustion gas properties calculated by method given in reference 7.

REFERENCES

1. Coffin, Kenneth P.: Burning Times of Magnesium Ribbons in Various Atmospheres. NACA TN 3332, 1954.
2. Markstein, George H.: Combustion of Metals. AIAA J., vol. 1, no. 3, Mar. 1963, pp. 550-552.
3. Gordon, A. S.; Drew, C. M.; Prentice, J. L.; and Knipe, R. H.: Techniques for the Study of the Combustion of Metals. AIAA J., vol. 6, no. 4, Apr. 1968, pp. 577-583.
4. Pinns, M. L.; Olson, W. T.; Barnett, H. C.; and Breitwieser, R.: NACA Research on Slurry Fuels. NACA Rep. 1388, 1958.
5. McAdams, William H.: Heat Transmission. Third ed., McGraw-Hill Book Co., Inc., 1954.
6. Maĉek, Andrej: Fundamentals of Combustion of Single Aluminum and Beryllium Particles. Eleventh Symposium (International) on Combustion. Combustion Institute, 1967, pp. 203-217.
7. Zeleznik, Frank J.; and Gordon, Sanford: A General IBM 704 or 7090 Computer Program for Computation of Chemical Equilibrium Compositions, Rocket Performance, and Chapman-Jouguet Detonations. NASA TN D-1454, 1962.

NASA-Langley, 1970 —— 27 E-5719

"The aeronautical and space activities of the United States shall be conducted so as to contribute . . . to the expansion of human knowledge of phenomena in the atmosphere and space. The Administration shall provide for the widest practicable and appropriate dissemination of information concerning its activities and the results thereof."

—NATIONAL AERONAUTICS AND SPACE ACT OF 1958

NASA SCIENTIFIC AND TECHNICAL PUBLICATIONS

TECHNICAL REPORTS: Scientific and technical information considered important, complete, and a lasting contribution to existing knowledge.

TECHNICAL NOTES: Information less broad in scope but nevertheless of importance as a contribution to existing knowledge.

TECHNICAL MEMORANDUMS: Information receiving limited distribution because of preliminary data, security classification, or other reasons.

CONTRACTOR REPORTS: Scientific and technical information generated under a NASA contract or grant and considered an important contribution to existing knowledge.

TECHNICAL TRANSLATIONS: Information published in a foreign language considered to merit NASA distribution in English.

SPECIAL PUBLICATIONS: Information derived from or of value to NASA activities. Publications include conference proceedings, monographs, data compilations, handbooks, sourcebooks, and special bibliographies.

TECHNOLOGY UTILIZATION PUBLICATIONS: Information on technology used by NASA that may be of particular interest in commercial and other non-aerospace applications. Publications include Tech Briefs, Technology Utilization Reports and Notes, and Technology Surveys.

Details on the availability of these publications may be obtained from:

SCIENTIFIC AND TECHNICAL INFORMATION DIVISION

NATIONAL AERONAUTICS AND SPACE ADMINISTRATION

Washington, D.C. 20546